Quantitative Analysis of Breast Skin for Tumor Detection Using Electromagnetic Waves

[1]D. A. Woten and [2]M. El-Shenawee

[1] Microelectronics-Photonics Program
dwoten@uark.edu
[2] Electrical Engineering Department, University of Arkansas
Fayetteville, Arkansas 72701

Abstract – This paper supplements the existing knowledge on the breast skin's effect on microwaves for tumor detection in the frequency range 4GHz - 7GHz. A realistic breast model is developed using data of an MRI scan of a physical breast. The breast fibro glandular content along with the tumor's size and location are considered. Numerical results indicate that the skin and tumor signatures could be on the same order of magnitude. This confirms the need to include the skin layer in breast models to minimize the potential of false alarms in tumor detection.

Keywords: Breast model, cancer detection, skin signature, and electromagnetic waves.

I. INTRODUCTION

Breast skin causes inevitable clutter when utilizing electromagnetic waves for cancer detection. In spite of its thickness being only a few millimeters, the skin can obscure the tumor signature. Studies published by radiologists showed that the skin thickness changes as a result of breast abnormalities, complicating the issue further [1]. For microwave imaging, incorporating the skin layer can represent a challenge when implementing computational techniques. These challenges include modeling the complex breast shape along with the varying skin thickness and the corresponding CPU time requirements for simulation.

Existing works addressing the skin simplify the problem in a number of ways. These simplifications include treating the breast as a two-dimensional model [2-7], simplifying the interior and exterior geometries [2-7] and utilizing ideal sources [2-8]. Two-dimensional models treat the breast as continuous flat layers or symmetric shapes which allow the closed form solutions for layered mediums to be utilized, while other simplifications include circular or cylindrical geometries in two or three dimensions [2-6]. In addition plane wave or dipole sources are typically utilized [2-7]. At this time, no single paper has detailed the skin's effect for realistic configurations of the breast shape, interior structure and practical antenna sources. This purpose of this work is to supplement the existing literature on breast skin effect in the microwave region using a realistic breast shape, interior structure and sources.

El-Shenawee *et al.* showed that the shape reconstruction of breast tumors in three dimensions using gradient methods required up to 26 CPU hours on a 64-bit machine, even though the skin layer was ignored [9]. In another previous study the breast was modeled as a coated sphere to incorporate the skin layer using the Mie Solution [7]. In that work, the error due to ignoring the skin layer was shown to be 3% when receiving in the backscatter direction, versus 30% when receiving in the forward direction. However, that work was preliminary and did not investigate the fibro glandular content, tumor size and location, realistic breast shape or practical sensors.

Human breast skin varies in thickness in each of the four regions of superior, inferior, medial and lateral shown in Fig. 1. The skin tends to be the thickest in the inferior region and thinnest in the lateral region [1]. Utilizing the experimentally acquired data reported in [1] and the fibro glandular interior structure obtained from a patient's MRI scan in [10] allows a realistic breast model to be generated. Broadband planar antennas are used for excitation to calculate the signature of the skin and the breast tumor as will be discussed in the following sections.

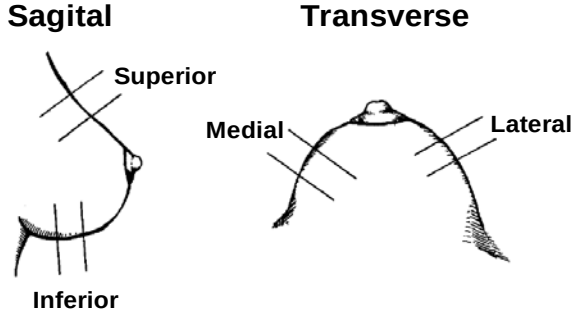

Fig. 1. The four regions of the breast.

II. METHODOLOGY

A. Development of Breast Model

As known, the human breast is a complex biological system containing fatty tissue, ducts, lobules and other fibro glandular tissue. All of these tissues are contained in a nonsymmetrical exterior shape of diverse proportions and a skin layer of varying thickness. To prove the concept of microwave imaging and detection of breast tumors, in the past few years, a variety of simplifications for the breast shape and interior structure were utilized in the literature [2-9, 11].

In this work, the breast model is assumed to contain five homogeneous regions as shown in Fig. 2(a). The interior regions correspond to the fatty breast tissue and the fibro glandular tissue representing the ducts, lobules, fat, etc. Taking 70 cross-sections of each region of the MRI scan allows for the creation of a three-dimensional configuration. Due to the lack of available 3D MRI scan data, we assume circular symmetry for the cross-section of each region shown in Fig. 2(a). For example, the cross-section a-a´ is shown in Fig. 2(b) and cross-section b-b´ is shown in Fig. 2(c). In this work, the skin layer is chosen to correspond to the values measured by Lee *et al.* [1]. Normal values of skin thickness are used in Figs. 2 to 6, while Fig. 7 shows results of minimum and maximum skin thickness. Normal skin thickness are 1.5mm for the superior region, 1.7mm for the inferior region, 1.5mm for the medial region and 1.3mm for the lateral region. The reported data ranges from 0.75 to 2.3mm for the superior region, from 0.7 to 2.7mm for the inferior region, from 0.6 to 2.4mm for the medial region and from 0.5 to 2.1mm for the lateral region. Outside the breast, a matching medium of oil with $\varepsilon_r = 3$ is assumed [12].

Recent measured electrical properties of breast tissues are reported in [13]. The new reported properties of the fibro glandular region are not significantly different from that of the malignant tumor (up to ~10% difference). However, a high contrast was reported to exist between the fatty and tumor tissues (~500%) [13].

The breast model used in this study incorporates the skin with varying thicknesses and with a permittivity of 36 and conductivity of 4 S/m, as reported at 6 GHz in [14]. Frequency dependence is incorporated in the imaginary part of the dielectric constant as reported in [7]. It is important to emphasize that skin thickness, fibro glandular content and tissue properties vary between patients based on physical and hormonal parameters [15].

B. Excitation Source

A three-element array of broadband planar antennas is designed in an effort to focus the beam on the tumor. The array operates between 4GHz and 7GHZ when immersed in oil. The array produces a beam focused directly above the central antennas as described in [11], [16]. The S_{11} of the antenna array shows that the maximum power is radiated at ~5GHz (not presented here but in [16]). The complex input impedance is around ~54+j4Ω between 4GHz and 7GHz. The antenna array is excited with 100mW input power with the complete design description reported in [11, 16].

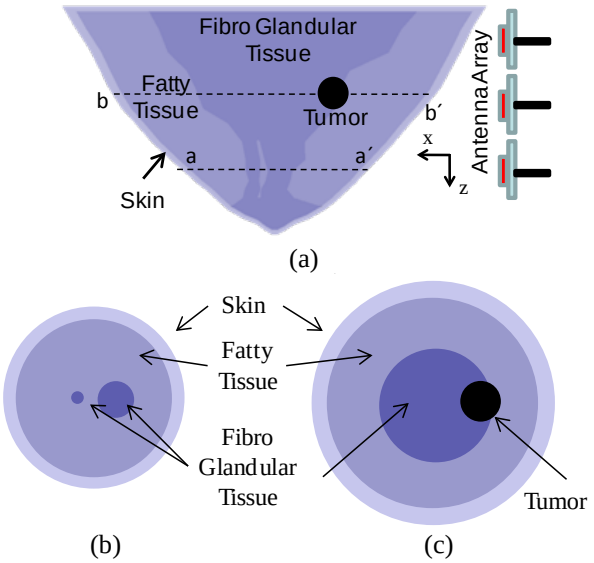

Fig. 2. (a) Breast model developed from MRI scan from [4] with tumor and antenna array, (b) top view of cross-section a-a´, and (c) top view of cross-section b-b´.

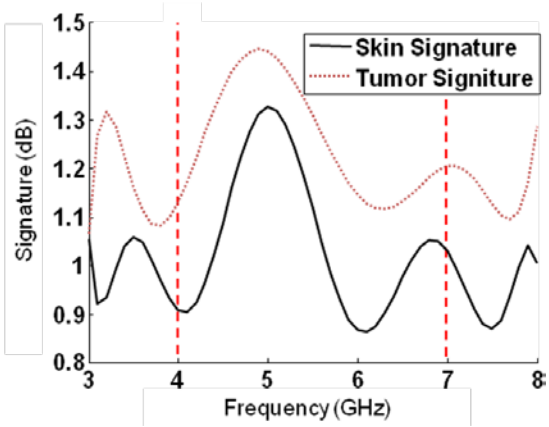

Fig. 3. Skin and tumor signatures for the 100% fibro configuration case. Tumor is located at (6, 0, 0) in Fig. 2(a).

C. Simulations

Integrating the breast model with the broadband array allows for the calculation of realistic skin and tumor signatures. The Ansoft HFSS package is used in this work. The signatures of the skin and tumor are referenced to the S_{11} parameter and are obtained by subtraction for the sake of analysis and comparison. For example, the skin signature was obtained upon subtracting the S_{11} of

the whole breast without a skin layer from the S_{11} with a skin layer ($S_{11(Breast+Skin)} - S_{11(Breast)}$). Similarly the tumor signature is calculated by subtracting the S_{11} of the whole breast without a tumor from the S_{11} of the breast and tumor ($S_{11(Breast+Skin+Tumor)} - S_{11(Breast+Skin)}$). The interior breast configuration is varied upon reducing the fibro glandular content while keeping the external breast shape, size, and electrical properties unchanged. The tumor size and location are also varied while keeping its electrical properties unchanged. The complex electrical parameters of breast tissues are obtained using the Cole-Cole curves in [13]. The fibro glandular tissue percentage shown in Fig. 2(a) will be referred to as the 100% fibro case, while a 75% fibro case would represent the same breast shape and size but with the fibro content decreased 25% by radial scaling.

The permittivity and conductivity of the fibro glandular and fatty tissue are reported for a range of frequency from 1-20GHz in [13]. For example, at 5GHz these values are 46 and 4 S/m, respectively, for the fibro glandular tissue and 6 and 1 S/m, respectively, for the fatty tissue [13].

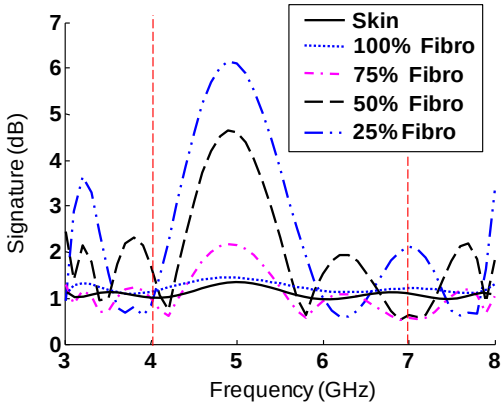

Fig. 4. Skin and tumor signatures for 100%, 75%, 50% and 25% fibro configurations. Tumor is located at (6,0,0) as in Fig. 2(a).

III. NUMERICAL RESULTS AND DISCUSSION

In the first case, the tumor is located at 4cm from the skin as shown in Fig. 2(a). The figure shows that the tumor partially overlaps the fibro glandular and the fatty tissue. The tumor is 10mm in diameter and is located in the direction of the main beam of the antenna array. Figure 3 shows the computed skin and tumor signatures vs. the frequency for 3-8GHz. The signature of the skin and tumor display an oscillatory behavior where the skin signature is smaller than that of the tumor. The difference between the skin and tumor signature is ~0.11dB at 5GHz. These oscillations could be due to the fluctuations in the radiation pattern as a function of the frequency (not shown here but in [16]). In [16], the radiation pattern showed that the side lobes were significant at some frequencies while disappeared at others.

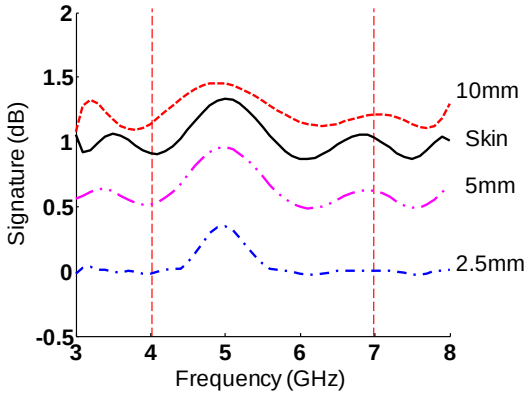

Fig. 5. Skin and tumor signatures for a tumor of diameter 10mm, 5mm and 2.5mm located at (6, 0, 0) in Fig. 2(a).

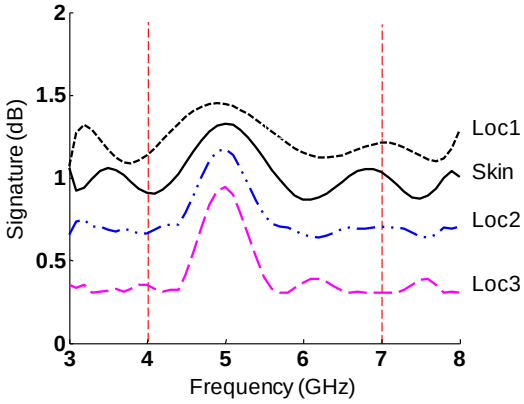

Fig. 6. Skin and tumor signatures for three locations; Loc1: (6,0,0), Loc2: (6,3,0), Loc3: (6,0,3) in Fig. 2(a).

In the second case, the fibro glandular content is reduced to 75%, 50%, and 25% as explained earlier. Accordingly, the tumor gradually changes from being partially overlapping the fibro glandular and fatty tissue (the 100% fibro case) to being totally immersed in the fatty tissue (the 25% fibro case). It is observed that the skin signature, obtained by subtraction, remains almost unvaried regardless of the fibro glandular content.

Figure 4 shows the skin signature vs. that of the tumor for the 100%, 75%, 50%, and 25% fibro content cases. The results show that the skin signature is the smallest in this case. In addition, as the content of fibro glandular tissue decreases, the tumor signature increases up to 6.25 dB for the 25% fibro case. These are anticipated results since with less fibro glandular tissue and more fatty tissue, the contrast between the tumor and surroundings increases leading to larger signature as shown in Fig. 4. This can be explained because the tumor has a higher contrast with the surrounding fatty tissue

(~500%) [13]. The maximum difference between the skin and tumor signatures is observed as ~5.12dB at 5GHz for the 25% fibro case as shown in Fig. 4.

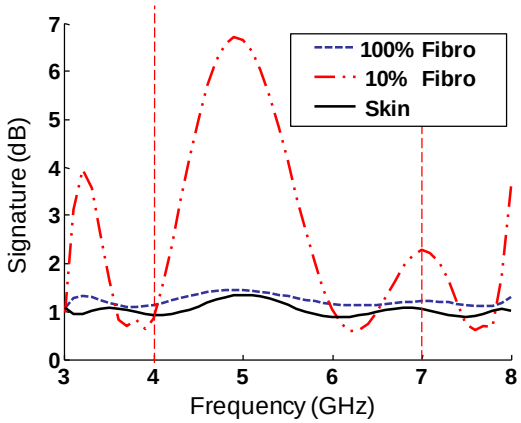

Fig. 7. Skin and tumor signatures for a 10mm tumor.

The third case varies the tumor size while utilizing the original fibro glandular content of 100% in Fig. 1. The diameter of the tumor is varied as 10mm, 5mm and 2.5mm as shown in Fig. 5. It is interesting to note that the skin signature, i.e. the clutter, could dominate the received signal. In other words, the skin signature is larger than that of the tumor of diameters 2.5 mm and 5 mm, in this case. In addition, the signature of a 10 mm tumor differs by only ~0.1dB to that of the skin as shown in Fig. 5.

The fourth case of Fig. 6 investigates the tumor location. As known, the ductal carcinoma in-situ is the most common breast cancer and can form at any location in the vast duct system. Thus, three possible tumor locations are tested in this figure at (6, 0, 0), (6, 3, 0) and (6, 0, 3). The second location, offset in the *y*-direction, is still in the direction of the main beam of the array while the third location, offset in the *z*-direction, is outside the direction of the main beam. The results of Fig. 6 show that when the tumor is located at Loc2 (6, 3, 0) and Loc3 (6, 0, 3), the skin signature is larger than that of the tumor. The tumor signature at Loc1 is only 0.1dB larger than that of the skin while it is 0.14dB and 0.49dB smaller than the skin signature for Loc2 and Loc3, respectively.

Figure 7 summarizes the extreme cases which could be encountered in reality. The 100% fibro content case in Fig. 2(a) could represent a younger woman with a dense breast. However, the process of menopause increases the relative fat content of the breast, and to represent this, a case with the fibro glandular content of only 10% is considered. Figure 7 depicts the skin signature vs. that of the tumor for these two fibro glandular contents using a 10mm diameter tumor.

The results of Fig 7 show that the 10mm tumor has a signature larger than that of the skin regardless of the fibro glandular tissue content. The maximum difference between the two signatures is shown in Fig. 8 to be ~5.4dB, i.e. ~6 times larger than the skin signature. However, the signature of a 2.5mm tumor is less than that of the skin, regardless of the fibro glandular content (result not shown). The difference is observed to be ~0.73dB and 1.09dB for the 10% and 100% fibro contents, respectively. The signature of smaller tumors could be theoretically increased when higher frequencies are used, but in reality the penetration depth of the waves will decrease, as expected.

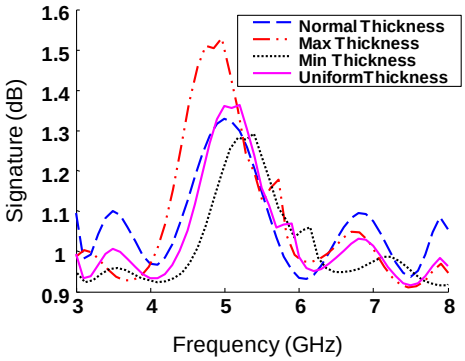

Fig. 8. Skin signatures for several thicknesses with the same breast interior contents. No tumor is included here.

In all above results, it is observed that the skin signature does not significantly change with respect to the interior structure of the breast (mainly the fibro glandular tissue). It is noticed that regardless of the fibro glandular content, tumor location, or size the skin signature is almost unchanged. Therefore, in all above figures, only one skin signature was plotted. This could be explained by the lossy nature of the breast tissue such that the effect of the multiple scattering between the tumor, fibro glandular tissue and the skin layer is diminished.

In all above results, the normal skin thickness reported in [1] was used. On the other hand, the results of Fig. 8 demonstrate the effect of the skin thickness. Figure 8 contains the skin thickness with normal thickness, maximum thickness (>2mm), minimum thickness (<0.7mm), and a uniform thickness of 1.5mm. The minimum and maximum ranges are mentioned in Section II as reported in [1]. The results show that the thickest skin layer has the largest signature, with a maximum of around 1.54dB vs. 1.3dB for the minimum thickness case. The maximum difference in the skin signatures between the thickest and thinnest skin layer is observed to be only ~0.24dB. The results of Fig. 7 indicate that a realistic skin signature could be approximately predicted by calculating the signature of a uniform skin layer of ~1-2mm thickness.

As known, it is almost impossible to predict the breast interior structure of a patient. However, the reconstruction of the exterior shape of the breast can be obtained as reported in [17]. Then a uniform skin layer could be engineered following the reconstructed breast shape in order to calculate its signature as shown in Fig. 8. Upon subtracting the predicted skin signature from the measurements of the signals scattered from the breast, the skin clutter can be removed. This process can help speeding up the computational algorithms for imaging the tumor. This process is expected to introduce some noise into the data, but less than a few dBs.

All above results were obtained using the HFSS package that required 20-24 CPU hours on a quad-core 64bit AMD Opteron workstation.

IV. CONCLUSIONS AND FUTURE WORK

The results of this work show that the signature of the skin could be comparable or even larger than that of the tumor depending on the fibro glandular content of the breast and the size and location of the tumor. This work confirms the importance of accounting for the skin layer in breast cancer detection at the microwave frequency range.

The current breast model can be improved by treating the fibro glandular region of the breast as discrete inclusions instead of a continuous region to incorporate the more heterogeneous nature of breast tissue. However, modeling individual duct systems and lobules along with the vascular system is computationally challenging due to their complex nature and minute feature sizes as reported in [18].

ACKNOWLEDGEMENTS

This work was supported in part by the NSF Graduate Research Fellowship, NSF GK-12 Program, NSF Award Number ECS – 0524042, the Arkansas Biosciences Institute (ABI), and the Women's Giving Circle at the University of Arkansas.

REFERENCES

[1] T. Lee, M. E. Read, and T. Medsker, "Breast skin thickness: normal range and causes of thickening shown on film –screen mammography," *Journal of Canadian Association of Radiologists*, vol. 35, pp. 365-68, Dec. 1984.

[2] E. Alanen and I. V. Lindell, "Effect of skin in microwave detection of breast cancer," *IEEE Trans. Microwave Theory and Techniques*, vol. 34, no. 5 pp. 584-588, May 1986.

[3] T. C. Williams, E. C. Fear, and D. T. Westwick, "Tissue sensing adaptive radar for breast cancer diction-investigations of an improved skin-sensing method," *IEEE Trans. Microwave Theory and Techniques*, vol. 54, no. 4, part 1, pp. 1308-1314, Jun. 2006.

[4] G. Wang and X. Zeng, "Impact of dispersion in breast tissue on high-resolution microwave imaging for early breast tumor detection," *IEEE Antennas and Propagation Society International Symposium*, vol. 3, pp. 2452-2455, Jun 2004.

[5] T. Williams, E. C. Fear, and D. W. Westwick, "Tissue sensing adaptive radar for breast cancer detection: investigations of reflections from the skin," *IEEE Antennas and Propagation Society International Symposium*, vol. 3, pp. 2436-2439, June 2004.

[6] M. Popovic and A. Taflove, "Two-dimensional FDTD inverse-scattering scheme for determination of near-surface material properties at microwave frequencies," *IEEE Trans. Antennas and Propagation*, vol. 52, no. 9, pp. 2366-2373, Sept. 2004.

[7] S. Pandalraju, "A hybrid algorithm based on Mie theory and evolution strategy for breast cancer imaging," M.S. Thesis, University of Arkansas, Fayetteville, AR, USA, 2006.

[8] T. C. Williams, J. M. Sill, and E. C. Fear, "Breast surface estimation for radar-based breast imaging systems," *IEEE Trans. Biomedical Engineering*, vol. 55, no. 6, pp. 1678-1686, June 2008.

[9] M. El-Shenawee and E. Miller, "Spherical harmonics microwave algorithm for shape and location reconstruction of breast cancer tumor," *IEEE Transaction on Medical Imaging*, vol. 25, pp. 1258-1271, Oct. 2006.

[10] R. Weisskoff, "MRImages," *int.ch.liv.ac.uk*, [Online].Available:http://int.ch.liv.ac.uk/Lanthanide/Ln_Chemistry_folder/MRI%20folder/MRImages.html. [Accessed Nov. 30, 2007].

[11] D. Woten, "Artificial neural networks for breast cancer detection using micro antennas," M.S. Thesis, University of Arkansas, Fayetteville, AR, USA, 2007.

[12] J. M. Sill and E. C. Fear, "Tissue sensing adaptive radar for breast cancer detection: study of immersion liquids," *Electronics Letters*, vol. 41, pp. 113-115, Feb. 2005.

[13] M. Lazebnik, D. Popovic, L. McCartney, C. B. Watkins, M. J. Lindstrom, J. Harter, S. Sewall, T. Ogilvie, A. Magliocco, T. M. Breslin, W. Temple, D. Mew, J. H. Booske, M. Okoniewski, and S. C. Hagness, "A large-scale study of the ultrawideband microwave dielectric properties of normal, benign, and malignant breast tissues obtained from cancer surgeries," *Physics in Medicine and Biology*, vol. 52, pp. 6093-6115, 2007.

[14] X. Li and S. C. Hagness, "A confocal microwave imaging algorithm for breast cancer detection," *IEEE Microwave and Wireless Components Letters*, vol. 11, no. 3, Mar. 2001.

[15] H. Ulger, N. Erdogan, S. Kumanlioglu, and E. Unur, "Effect of age, breast size, menopausal and hormonal status on mammographic skin thickness," *Skin Research and Technology*, pp. 284-289, 2003.

[16] D. A. Woten and M. El-Shenawee, "Broadband dual linear polarized antenna for statistical detection of breast cancer," *IEEE Antenna and Propagation Letters*, vol. 56, no. 11, Nov. 2008

[17] M. R. Hajihashemi and M. El-Shenawee, "Breast Shape Reconstruction using Microwave Techniques and The Level Set Method," , *24th Annual Review of Progress in Applied Computational Electromagnetics*, Niagara Falls, Canada, pp. 98-103, Mar. 2008.

[18] J. Greenlee, S. Shumate, and M. El-Shenawee, "A comprehensive approach to modeling breast cancer," *Proc. Ohio Collaborative Conference on Bioinformatics*, Toledo, Ohio, June 2-4, 2008.

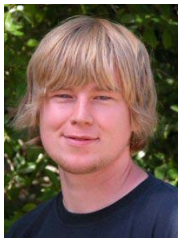

Douglas A. Woten received the B.A. degree with honors in mathematics and the B.A. in physics from Hendrix College, Conway, AR in 2005. He received the M.S. degree in Microelectronics-Photonics from the University of Arkansas in 2007 and is currently pursuing his Ph.D. in the same program. He is a recipient of the National Science Foundation (NSF) Graduate Research Fellowship and two time recipient of the NSF GK-12 Fellowship.

Magda El-Shenawee (M'91) received the B.S. and M.S. degrees in electrical engineering from Assiut University, Assiut, Egypt, and the Ph.D. degree in electrical engineering from the University of Nebraska-Lincoln in 1991. In 1992, she worked as a Research Associate in the Center for Electro-Optics at the University of Nebraska where she focused on the problem of enhanced backscatter phenomena. In 1994 she worked as a Research Associate at the National Research Center, Cairo, Egypt, and in 1997, she worked as Visiting Scholar at the University of Illinois at Urbana-Champaign. In 1999, she joined the MURI team (Multidisciplinary University Research Initiative) at Northeastern University, Boston. Currently, Dr. El-Shenawee is an Associate Professor in the Department of Electrical Engineering at the University of Arkansas, Fayetteville. Her research areas are microwave imaging of breast cancer, computational inverse problems, microwave imaging systems, mathematical biology of breast tumors, MEMS antennas, biophysics of tumors, rough surface scattering, computational electromagnetics, subsurface sensing of buried objects, landmine detection, and numerical methods for microstrip circuits. Dr. El-Shenawee is a member of Eta Kappa Nu electrical engineering honor society.